RESEARCH PAPER

Acta Neurobiol Exp 2020, 80: 305–321
DOI: 10.21307/ane-2020-027

Phenylbutyrate administration reduces changes in the cerebellar Purkinje cells population in PDC-deficient mice

Ilona Klejbor[1,2,4], Saleh Mahmood[1], Natalia Melka[2], Adriana Ebertowska[2], Janusz Morys[2], Ewa K. Stachowiak[3], Michal K. Stachowiak[3] and Mulchand S. Patel[1]*

[1] Department of Biochemistry, Jacobs School of Medicine and Biomedical Sciences, University at Buffalo, Buffalo, NY, USA, [2] Department of Anatomy and Neurobiology, Medical University of Gdansk, Gdansk, Poland, [3] Department of Pathology and Anatomical Sciences, Jacobs School of Medicine and Biomedical Sciences, University at Buffalo, Buffalo, NY, USA, [4] Department of Clinical Anatomy, Pomeranian University in Slupsk, Poland,
** Email: mspatel@buffalo.edu*

In humans, pyruvate dehydrogenase complex (PDC) deficiency impairs brain energy metabolism by reducing the availability of the functional acetyl-CoA pool. This "hypometabolic defect" results in congenital lactic acidosis and abnormalities of brain morphology and function, ranging from mild ataxia to profound psychomotor retardation. Our previous study showed reduction in total cell number and dendritic arbors in the cerebellar Purkinje cells in systemic PDC-deficient mice. Phenylbutyrate has been shown to increase PDC activity in cultured fibroblasts from PDC-deficient patients. Hence, we investigated the effects of postnatal (days 2-35) phenylbutyrate administration on the cerebellar Purkinje cell population in PDC-deficient female mice. Histological analyses of different regions of cerebellar cortex from the brain-specific PDC-deficient saline-injected mice revealed statistically significant reduction in the Purkinje cell density and increased cell size of the individual Purkinje cell soma compared to control PDC-normal, saline-injected group. Administration of phenylbutyrate to control mice did not cause significant changes in the Purkinje cell density and cell size in the studied regions. In contrast, administration of phenylbutyrate variably lessened the ill effects of PDC deficiency on Purkinje cell populations in different areas of the cerebellum. Our results lend further support for the possible use of phenylbutyrate as a potential treatment for PDC deficiency.

Key words: pyruvate dehydrogenase complex deficiency, cerebellum, Purkinje cells, phenylbutyrate, mouse model

INTRODUCTION

The human brain is a highly energy-consuming organ. It accounts for about 2% of body weight in adults, but in resting conditions, it consumes as much as 20% of the total oxygen. Maintaining the brain energy homeostasis is a very complex process due to the sensitivity of neurons to metabolic stress and the fact that, unlike other tissues, glucose serves as the primary oxidizable substrate for the brain (Sokoloff, 1999; Jankowska-Kulawy et al., 2014). Pyruvate dehydrogenase complex (PDC) plays a crucial role in oxidation of glucose by connecting the glycolytic pathway with the tricarboxylic acid cycle (Patel and Roche, 1990). The activity of PDC in brain structures is several times higher than in other tissues, ensuring a continuously high level of acetyl-CoA production (Jankowska-Kulawy et al., 2014). Phosphorylation of the α subunit of the pyruvate dehydrogenase (PDH) component of the PDC by PDH kinases inactivates this complex whereas dephosphorylation by PDH phosphatases restores PDC activity (Patel and Roche, 1990; Hemalatha et al., 1995; Patel and Harris, 1995; Harris et al., 2002; Patel and Korotchkina, 2003).

Received 14 February 2020, accepted 8 June 2020

© 2020 by Acta Neurobiologiae Experimentalis

In humans, deficiency of PDC resulting from mutations in the component proteins impairs brain energy metabolism by reducing the availability of the functional acetyl-CoA pool. Therefore, this "hypometabolic defect" results in congenital lactic acidosis and abnormalities of brain morphology and function (Patel et al., 1992; Matthews et al., 1994; Rubio-Gozalbo et al., 1999; Triepels et al., 1999; Lissens et al., 2000; Robinson, 2001; 2006). Among various neurological dysfunctions observed in patients with PDC deficiency, cerebellar symptoms from mild ataxia to profound psychomotor retardation often have been reported (Brown et al., 1994; Cross et al., 1994; De Meirleir, 2013; DeBrosse and Kerr, 2016).

The cerebellum is usually defined as a key structure in sensory-motor processing. For higher-level motor, cognitive and behavioral tasks, the cerebellum provides modulatory function *via* loops with sensorimotor, association, and limbic regions of the cerebral cortex (Voogd and Glickstein, 1998; Middleton and Strick, 2001; Kelly and Strick, 2003; Schmahmann, 2004; Schmahmann et al., 2007; Buckner, 2013). Evidence from affected children (Levisohn et al. 2000), imaging studies in humans (Grodd et al., 2001; Wildgruber et al., 2001; Grodd et al., 2005) and clinical reports (Tavano et al., 2007) provide support for the notion that the cerebellum is an essential structure to create and regulate neuronal connections involved in motor control as well as in emotion (Leggio and Olivito, 2018; Stoodley and Schmahmann, 2018).

Purkinje cells (PCs) are a key, GABAergic, inhibitory neurons, located as the single row between granular and molecular layer of the cerebellar cortex, characterized by unique fan-shaped dendritic trees extended into the molecular layer. PCs receive excitatory inputs from climbing fibers and parallel fibers as well as inhibitory inputs from both stellate and basket cells. On the other hand, the myelinated axons of the PCs send inhibitory signals to the deep cerebellar nuclei and certain brainstem nuclei, which control the final output of the cerebellum (Reeber et al., 2013a; 2013b; White and Sillitoe, 2013; Leto et al., 2016). The fundamental organization of the cerebellar cortex architecture is based on its subdivision into functional transverse zones and parasagittal stripes (Apps and Hawkes, 2009; Jankowski et al., 2011; Leto et al., 2016; Apps et al., 2018). The cerebellar compartmentation is determined mainly by intrinsic differences between subsets of PCs as well as the pattern of afferent and efferent connections (Leto et al., 2016). Specification of the PC subtype probably occurs when PCs undergo terminal mitosis between E10 and E13 (Miale and Sidman, 1961; Leto et al., 2016) and start migrating to their destinations in the cerebellum of mice (Yuasa et al., 1991; Komuro, 2013). Development studies have shown two distinct PC populations. An 'early-born' PC population predominantly born in the posterior region of ventricular zone migrates to the nascent PC plate by E14.5. These cells utilize a tangential migratory pathway. The second population consisting of the 'later-born' PCs migrates to more laterally located parts of the cerebellum than the 'early-born' counterparts utilizing a radial glial scaffold away from ventricular zone. 'Early'- and 'later-born' PCs have distinct molecular characteristic (White and Sillitoe, 2013). One of the specific markers of PC's molecular heterogeneity is zebrin II (ZII). 'Early-born' PCs (E10–E11.5) are destined to become ZII^+ and 'later-born cells (E11.5–E13) remain as ZII^-. Furthermore, a direct correlation was also found between PCs birth-timing and their adult zones and stripes location, suggesting that both molecular heterogeneity (e.g., ZII^+ *vs.* ZII^-) and topographic information (zone or stripe) are acquired and that colonization of the final destination places is performed in strict order (Leto et al., 2016). As a consequence, in the adult cerebellum, the structures that were formed earlier in ontogenetic development, for example a vermis, are located in the middle and the structures formed later (cerebellar hemispheres) are located laterally.

In our previous study we showed a reduction in PCs density in adult (P-35) PDC-deficient female mice (with systemic PDC deficiency) in different cerebellar folia (Pliss et al., 2013). Moreover, PCs from PDC-deficient females demonstrated fewer and shorter dendritic processes with the fewer branches compared to PCs in cerebellar sections from age-matched control females. These findings clearly indicated an impairment in the PC dendritic arbor development in the PDC-deficient mice (Pliss et al., 2013).

Therapeutic strategies for the PDC deficiency are limited and are generally not very effective in improving neurological symptoms and clinical outcomes. The most widely used treatment has been starting a high-fat, ketogenic diet postnatally as early as possible after confirming the diagnosis of PDC deficiency. The rationale for this dietary treatment is to provide ketone bodies as an alternate fuel for brain metabolism in the fed state and also to curtail lactate production from glucose metabolism. The metabolism of ketone bodies to acetyl-CoA in the mitochondria bypasses the PDC reaction. Another commonly employed treatment for PDC deficiency is supplementation of pharmacological doses of thiamine for a possible increase in the availability of thiamine pyrophosphate as a cofactor for PDH. Thiamine therapy has been shown to be effective in only a very few 'thiamine-responsive" PDC-deficient patients with mutations in the *PDHA1* gene altering its Km for thiamine pyrophosphate. The less preferred

option for treatment is administration of dichloroacetate, a known inhibitor of PDH kinases. A fraction of the residual PDC protein in PDC-deficient patients is subject to phosphorylation/inactivation, further reducing the PDC function. Dichloroacetate treatment has been shown to increase PDC activity in cultured human fibroblasts and decrease lactate levels in cerebrospinal fluid from PDC-deficient patients (Shireman et al., 1984; Naito et al., 1988). However, dichloroacetate, is not commonly used as an extended treatment option for PDC deficiency due to its observed neurotoxicity (Kaufmann et al., 2006).

PDC-deficient patients usually have low but variable levels of residual PDC activity in all tissues but a portion of it is present as phosphorylated 'inactive' PDC. Phenylbutyrate has recently been shown to inhibit PDH kinases, resulting in reduction in the phosphorylated form of PDHα protein (thus increasing PDC activity) in tissues from normal adult mice injected with this inhibitor (Ferriero et al., 2013) and in fibroblasts from PDC-deficient patients (Ferriero et al., 2013). Phenylbutyrate treatment has also been shown to correct the retinal morphology, locomotor, and biochemical abnormalities in the noa^{m631} zebrafish model of PDC deficiency (Brockerhoff et al., 1995; 1998). Phenylbutyrate administration also reduced or prevented systemic lactic acidosis induced by partial hepatectomy, heart ischemia, septic shock, and stroke (Preiser et al., 1990; Ayala et al., 2012). A protective role of phenylbutyrate was shown during cerebral ischemia (Qi et al., 2004; Srinivasan and Sharma, 2011).

Our earlier study has shown malformation of the brain structures in developing mouse brain due to brain-specific PDC deficency (Pliss et al., 2004). In another study from our laboratory there was a depletion of the PCs in the cerebellum of systemic PDC-deficient female mice (Pliss et al., 2013). On the basis of these observations, we investigated the effect of phenylbutyrate administration during the immediate postnatal period on the development and maturation of the cerebellar PC population (density and size) in PDC-deficient mice.

METHODS

Generation of brain-specific PDH-deficient (aka PDC-deficient) female mice

A mouse line carrying two loxP sites inserted into introns surrounding exon 8 of the X-linked *Pdh*α1 gene (*Pdha1^{flox8}*) was reported previously (Johnson et al., 2001). This mouse line had a 129J genetic background. In our previous study we bred females (genetic background 129J, *Pdha1^{flox8}/Pdha1^{flox8}*) with nestin-Cre transgenic males (genetic background C57BL/6J, Nestin-Cre) from The Jackson Laboratory (Pliss et al., 2004; 2007). In these previously reported studies, the PDC-deficient female progeny of this breeding had a mixed genetic background (129J/B6). To overcome the possible contribution of this mixed genotype on the phenotype of the brain-specific PDC-deficient female progeny reported previously, floxed females (genotype 129J, *Pdha1^{flox8}/Pdha1^{flox8}*) were back-crossed for 10 generations with wild-type males (B6 genetic background). The progeny of the last breeding was intra-bred to derive a floxed colony (termed as 'B6-transferred') with B6 genetic background.

In the present study, to generate brain-specific PDC-deficient female mice, the floxed females from this B6-transferred colony were bred with the transgenic males {B6Cg[SJL]-TgN[NesCre]1Kln}(Cre^{br}) harboring a *Cre* transgene driven by the nestin promoter. To generate control, PDC normal mice, wild-type B6 females (*Pdha1^{wt}/Pdha1^{wt}*) were bred with transgenic *nestin-Cre* B6 males. Only Cre-positive females of this breeding were used as control. Both control and PDC-deficient female progenies were injected intraperitoneally with either sterile saline or phenylbutyrate (250 mg/kg body weight, Sigma-Aldrich) in sterile saline (Ferriero et al., 2013) once a day starting from postnatal day 2 to day 35 creating four treatment groups: control mice injected with saline (CSA), control mice injected with phenylbutyrate (CPB), experimental PDC-deficient mice injected with saline (ESA), and experimental PDC-deficient mice injected with phenylbutyrate (EPB). Their body weights were recorded daily for dose calculation. Progeny was weaned on a rodent chow and water *ad libitum* on postnatal day 21 but continued to receive their assigned daily treatment until postnatal day 35. Unless otherwise indicated, 35-day-old progeny females (~18 h after the last injection) were anaesthetized with ketamine (100 mg/kg) and xylazine (10 mg/kg) and either perfused to fix the brain for histological analyses or decapitated to collect blood and to harvest tissues (weighed and frozen immediately at -80°C) for biochemical analyses. Animal protocols were approved by the Institutional Animal Care and Use Committee of the State University of New York at Buffalo in accordance with the Guide for the Use and Care of Laboratory Animals. All animal studies (including breeding, postnatal care and treatments, euthanization, brain sectioning and biochemical analyses) were performed at the University at Buffalo, and staining and analyses of fixed cerebellar sections were performed at the Medical University of Gdansk.

Tail DNA for initial genotyping (around postnatal day 10) as well as DNA isolated from collected

tissues (brain and liver obtained at the time of killing) were genotyped as per manufacturer's protocol (OmniprepTM I, Genotechnology Inc). Genomic DNA was amplified using a *Pdha1* and *Cre* primers as reported previously (Pliss et al., 2004). The presence of three *Pdha1* alleles (*Pdha1*^{wt}, *Pdha1*^{flox8}, and *Pdha1*$^{\Delta ex8}$) and the *Cre* transgene was determined by polymerase chain reaction (PCR) analysis (Pliss et al., 2004).

qRT-PCR analysis

Brain *Pdha1* mRNA levels in PDC-deficient female mice were quantified using CFX96 Touch RT-PCR detection system (Bio-Rad). Total RNA was extracted from ~100 mg of frozen brain tissues using TRIzol Reagent (Life Technologies) according to the manufacturers' instruction and 1 µg of total RNA was reverse transcribed into cDNA using an iScript cDNA kit (Bio-Rad). Quantitative real time PCR reactions were performed using appropriately diluted cDNA in triplicate with β-actin serving as an internal control. Relative quantification of mRNA levels was analyzed using the $2^{-\Delta\Delta CT}$ method (Livak and Schmittgen, 2001). To generate a ΔCT value, data were normalized to β-actin and ΔΔCT values were obtained by normalizing data to mean ΔCT values of the control group. Following were the primers used for *Pdha1* and *β-actin* gene expression.
Pdha1 forward primer: 5'-TGGCAGCACTGTGGAAATTA-3',
Pdha1 reverse primer: 5'-CGCACAAGATATCCATTCCA-3';
β-actin forward primer: 5'-GCTCTTTTCCAGCCTTCCTT-3',
β-actin reverse primer: 5'-CTTCTGCATCCTGTCAGCAA-3'.

Western-blot analysis

Approximately 100 mg of brain (maintained at -80°C frozen) from 35-day-old PDC-deficient and control mice (18 h after the last injection of saline or phenylbutyrate) were homogenized in ice-cold lysis buffer (50 mM HEPES pH 8.0, 150 mM NaCl, 1 mM sodium orthovanadate, 30 mM sodium fluoride, 10 mM dichloroacetate, 10 mM sodium pyrophosphate, 10 mM EDTA, 1% Triton X-100). Protease inhibitor cocktail (5 µl/ml) (Sigma-Aldrich) and PMSF (1 mM) were added to this lysis buffer just before use. Brain lysate was extracted by centrifuging at 12000xg, for 15 min at 4°C. The supernatants were stored at -80°C. The protein content of the thawed solubilized tissue lysate was determined using Bio-Rad protein assay method according to their instruction. For western-blotting, 25-100 µg of proteins were analyzed by sodium dodecyl sulfate-polyacrylamide gel electrophoresis, transferred to nitrocellulose membrane and immunodetected by Enhanced Chemiluminescence kit (Perkin-Elmer) and analyzed using Bio-Rad ChemiDOC MP image analyzer. Following antibodies were used for Western blot analyses: anti-human PDH antibody (Pliss et al., 2013) (cross reacting with rodent PDH) to detect the α subunit of the PDH component of PDC; anti-phospho-human PDHE1-A type 1 (phosphor-Ser293) (EMD Millipore) (cross reacting with rodent PDH) to detect phosphoE1α; and human β-actin monoclonal antibody (D6A8) (Cell Signaling Technology) to detect β-actin used as loading control.

Morphological and stereological analyses

Four different groups of 35-day-old mice (as described above) were investigated: CSA (n=8), CPB (n=10), ESA (n=8) and EPB (n=5). Approximately eighteen h after the last phenylbutyrate or saline injection mice were anaesthetized with ketamine (100 mg/kg) and xylazine (10 mg/kg) and then perfused with 4% paraformaldehyde in the 0.1 M phosphate buffer saline at 4°C. Next, brains were removed, post-fixed for 2 h in the perfusing solution and then cryoprotected in 15% and 30% sucrose, respectively, for 24 h at 4°C each. Brains were cut into 40 µm thick coronal sections on a cryostat (Jung CM1800, Leica, Germany) and stored at -20° C for further processing.

Three sections were taken from each of the six regions of interest based on the Paxinos and Franklin stereotaxic atlas (Paxinos and Franklin, 2013). These sections were stained with cresyl violet, dried and cover-slipped. The delineation of subdivisions of the cerebellum were prepared using the subdivisions of vermis proposed by Apps and Hawkes (2009) and for cerebellar hemispheres by Paxinos and Franklin (2013). In order to estimate the quantitative changes of PCs in the cerebellar cortex, we subdivided the vermis into four zones: anterior zone (AZ contained lobules I-V); the central zone (CZ; lobules VI and VII); the posterior zone (PZ; lobule VIII and dorsal part lobule IX) and the nodular zone (NZ; ventral part lobule IX and lobule X) (Fig. 1). Cerebellar hemispheres were subdivided into: Crus1, Crus2, simple lobule, paramedian lobule (Fig. 1). We estimated: the number of profiles per millimeter of the PCs layer (N_L) and the mean area of profiles.

$$N_L(prof/line) = \frac{N(prof)}{L(lenght)} = \frac{number\ of\ profiles}{lenght\ of layer}$$

PCs were quantified using the images obtained from AxioScan.Z1 system (Zeiss, Germany) using the Zeiss Zen 2.3 (Blue Edition) Software. The image analysis

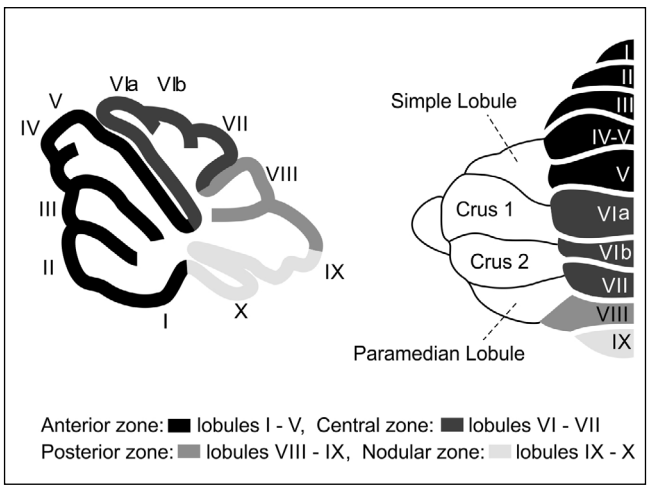

Fig. 1. Schematic diagram showing the subdivision of the cerebellum used in this study.

program Zen 2.3 (Blue Edition; Zeiss, Germany) - for light microscope image reconstruction was used. The recognition of the regions of interest was achieved at 4x lens and the profiles of cells were measured at 40x. The results were estimated from randomly distributed test areas covering the whole area of the studied brain region. Thirty to fifty test areas and 100-200 counted cells per region were taken from each animal.

Statistical analysis was carried out using GraphPad Prism version 8.00 for Mac, (GraphPad Software; www.graphpad.com). All data are presented as mean ± standard error. Unless otherwise indicated, groups of data were compared using ANOVA or MANOVA Fisher test followed by Tukey's multiple comparisons. Values of $p<0.05$ or lower were considered as significant.

RESULTS

Genotyping

The genotype analyses using tail DNA from control (CSA and CPB) and experimental PDC-deficient (ESA and EPB) female pups on postnatal day 10 verified the presence of *Pdha1*^{wt} and *Cre*$^{+}$ alleles and *Pdha1*^{wt}/*Pdha1*^{flox8} and *Cre*$^{+}$, respectively. In brain samples collected at the time of killing and frozen immediately at -80°C for biochemical analyses, we observed the presence of *Pdha1*^{wt} and *Cre*$^{+}$ in the CSA and CPB mice and *Pdha1*^{wt}/*Pdha1*$^{\Delta ex8}$ and *Cre*$^{+}$ in the ESA and EPB female mice (results not shown). These findings are similar to previously reported findings for control and PDC-deficient females from our lab (Pliss et al., 2004; 2013). Brain-specific deletion of the *Pdha1*^{floxed}-allele was supported by the absence of deletion of the *Pdha1*^{floxed}-allele in livers from ESA and EPB mice (results not shown). This finding is also similar to that reported previously for the brain-specific PDC-deficient female mice (Pliss et al., 2004).

Body and brain weight analysis

In the present study, female mice were divided into four treatment groups starting on the postnatal day 2 and their brains were collected on postnatal day 35. PDC-deficient female mice (ESA and EPB) grew at a normal rate during the first 15 days after birth but thereafter their growth nearly ceased (Fig. 2A). By postnatal 35, this group of mice weighed approximately 50% less compared to age-matched controls (CSA and CPB). On postnatal day 35, the body weight of the saline-injected control group (CSA; n=8) was 14.1±0.3 g and that of phenylbutyrate-injected control group (CPB; n=10) was 13.7±0.3 g (statistically non-significant difference). The body weights of the saline-injected experimental (PDC-deficient) group (ESA; n=8) (7.4±0.7 g; $p<0.001$) and the phenylbutyrate-injected experimental group (EPB; n=5) (8.4±0.5 g) were also significantly lower ($p<0.05$) compared to the CSA group (Fig. 2A-B). The results show that daily injection of phenylbutyrate had no significant effect on body weights of the control and PDC-deficient mice. We observed no mortality in the control CSA and CPB groups during the treatment period up to 35 days. We did observe modest mortality in severely PDC-deficient groups (22.2% for ESA and 15.4% for EPB; $p=0.9881$ using a Pearson chi-square test). In our previous studies, there was no mortality and no growth retardation of female mice (a mixed genetic background of 129J/B6) with a milder form of PDC deficiency (~20% reduction) (Pliss et al., 2004; 2013). In the present study, the 'B6-transferred' mouse model with B6 genetic background developed mild to severe PDC deficiency [a greater degree of deficiency (~50% reduction in PDHα protein level; see below), growth retardation (Fig. 2A), and modest mortality, representing a closer phenotype commonly observed in PDC-deficient patients.

Brain weight of PDC-deficient mice (ESA) was significantly lower (about 25%; $p<0.05$) compared to the control group (CSA) (0.32±0.01 g *vs.* 0.43±0.01 g, respectively) (Fig. 2C). There was no statistical difference in the brain weight between CSA and CPB groups (0.46±0.01 g and 0.43±0.01 g, respectively). The brain weight of PDC-deficient mice treated with phenylbutyrate (EPB) remained significantly lower (30%; $p<0.05$) than of the CSA mice (0.30±0.02 g *vs.* 0.46±0.01 g, respectively) (Fig. 2C). Additionally, there were no significant changes in the brain weight between ESA and EPB groups.

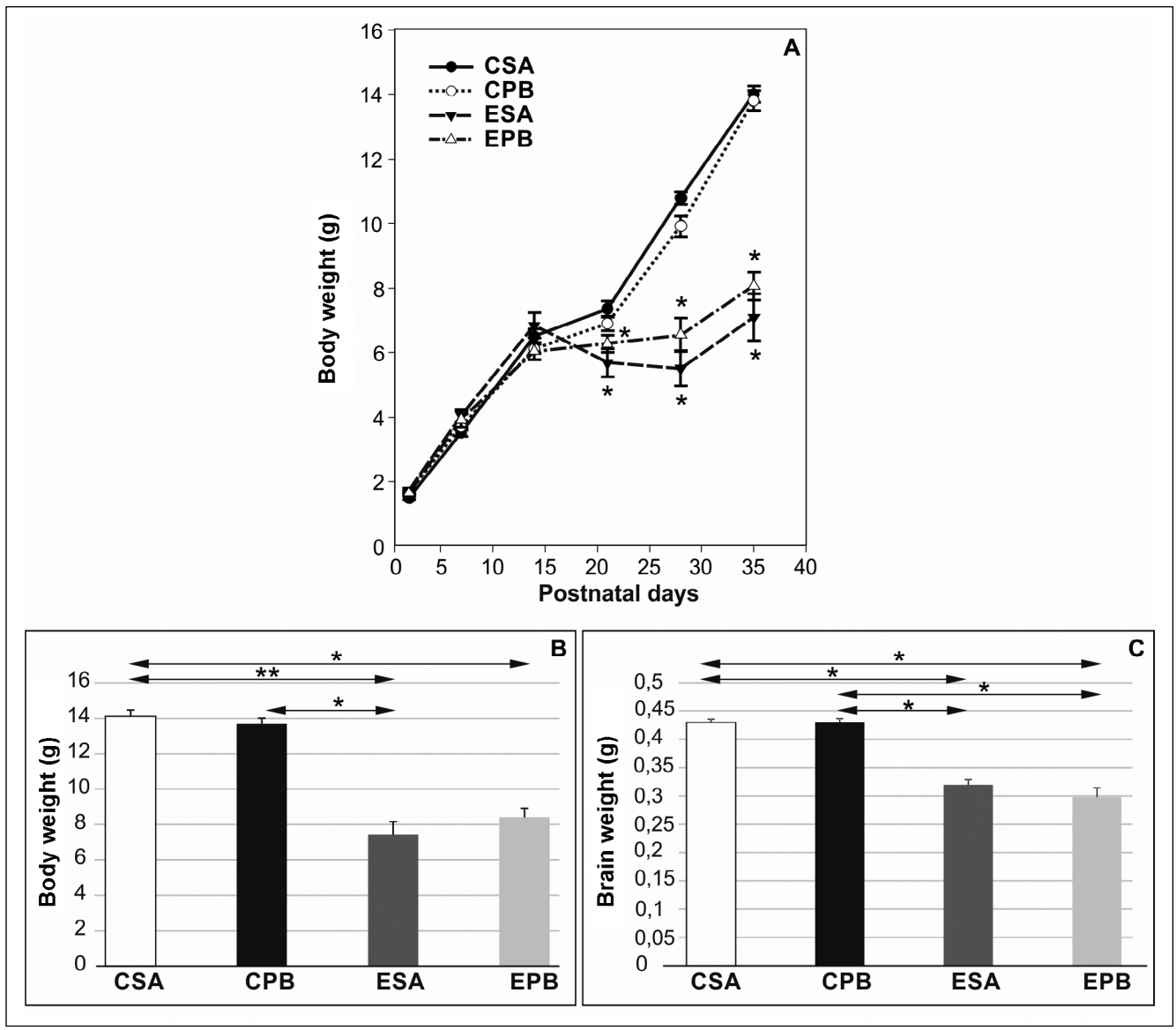

Fig. 2. Body and brain weights of control and PDC-deficient experimental female mice during the immediate postnatal life. Both control and PDC-deficient pups were injected intraperitoneally with either sterile saline (SA) or phenylbutyrate (PB) (250 mg/kg body weight) in sterile saline once a day starting from the postnatal day 2 to day 35, resulting in four treatment groups: CSA, CPB, ESA, and EPB. Mice were weaned on a standard lab chow and water ad libitum on the postnatal day 21 but continued to receive their assigned daily treatment until postnatal day 35 when they were euthanized to collect tissues. Growth of mice is shown in A. Significance was evaluated by Friedman test in four treatment groups: CSA (Friedman test = 459.66, N=14, df=33), CPB (Friedman test = 323.50, N=10, df=33), ESA (Friedman test = 250.94, N=12, df=33), and EPB (Friedman test = 304.50, N=10, df=33). Bar graphs show the average body (B) (Kruskal-Wallis test H (3, N=49) = 15.40) and brain (C) weights (grams) (Kruskal-Wallis test H (3, N=49) = 37.10) of four groups of 35-day-old mice. Data are means ± S.E. (n=5-10), * represents p<0.05, ** represents p<0.001.

PDHα mRNA and protein levels in brain tissues

There was a significant reduction in the level of PDHα mRNA in brains of PDC-deficient (ESA) mice compared to that of the control (CSA) mice (Fig. 3A). As expected based on heterozygous status of affected females, there was a significant reduction (about 50%) in the total PDHα protein (E1) level in brains of PDC-deficient (ESA) mice compared to control (CSA) mice (Fig. 3B). However, phenylbutyrate injection had no effect on the levels of either the total PDHα protein (E1) (results not shown) or phosphorylated PDHα protein (PE1) in brains from both the groups of mice (Fig. 3C-D), indicating that this treatment had no significant effect on reducing the levels of phospho-PDHα protein (PE1) in the brains. This treatment, however, did decrease the levels of phospho-PDHα protein in liver homogenates (results not shown), indicating that

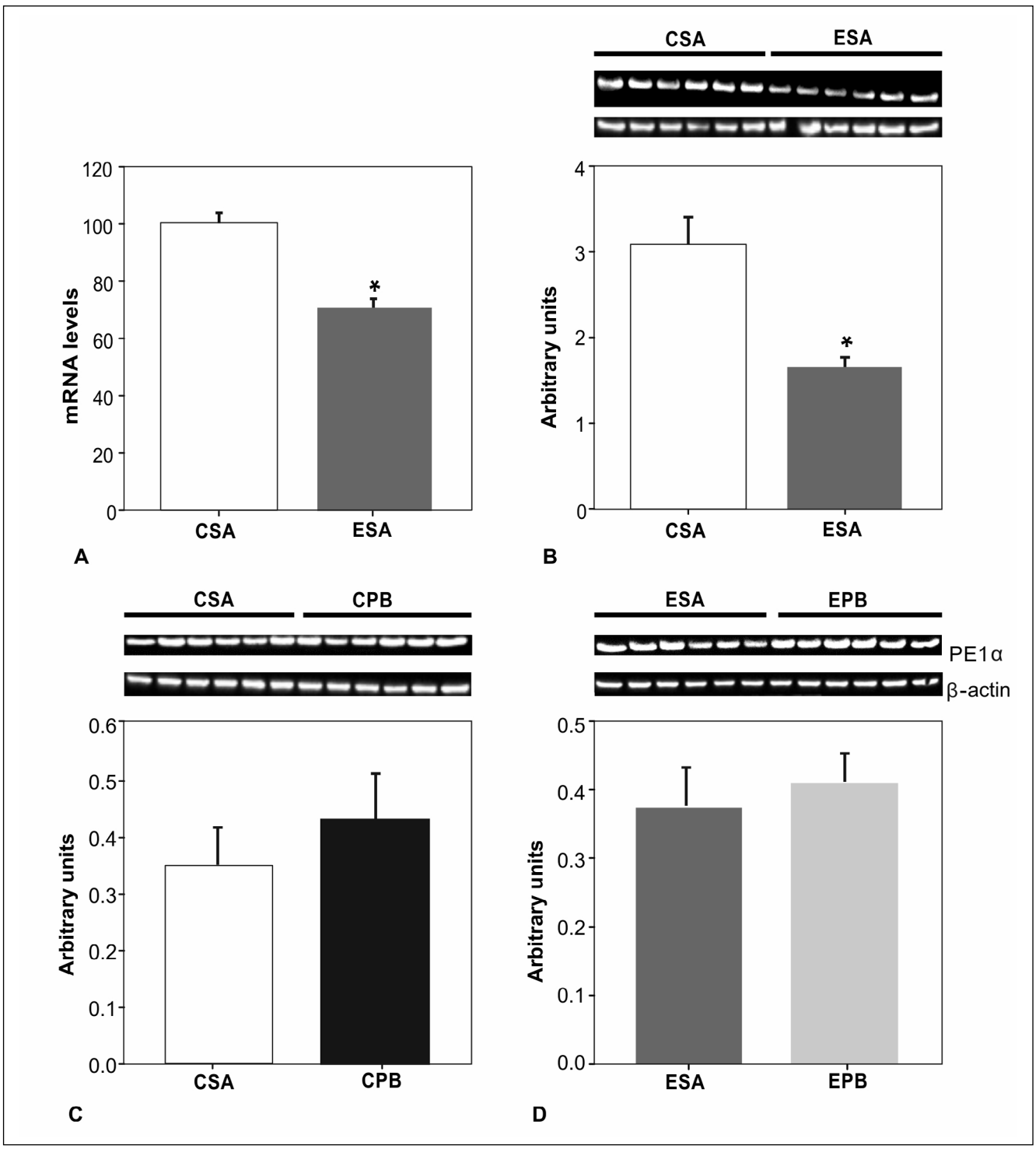

Fig. 3. *Pdha1* mRNA and PDH protein analyses in brains from 35-day-old control and PDC-deficient mice. Both the groups of mice received either saline or phenylbutyrate treatments from day 2 to 35, resulting in four treatment groups: CSA, CPB, ESA, and EPB. (A) Total RNA was extracted from brain and mRNA levels were quantified by qRT-PCR with β-actin mRNA used as an internal control. Individual samples were run in triplicate and results are expressed as means ± SE (n=6-8/group; *p<0.05 using Student's t test as explained below). For western blot analysis, brain homogenates were prepared and separated proteins were detected with either E1α antibody or phosphoE1α antibody, and β-actin antibody served as loading control. (B) Comparison of E1α (total) protein levels between the saline-injected control (CSA) and PDC-deficient (ESA) mice and (C) comparison of phosphoE1α (PE1α) protein levels between the CSA and CPB, and (D) between ESA and EPB mice. The results of samples from two groups of mice (as identified in figures above) performed either in the same qRT-PCR amplification or western blot gel were directly compared using Student's t test. Results are normalized with β-actin and expressed as means ± SE (n=6, * represents p<0.05).

the treatment was effective in the liver but not in the brain. In this experiment, mice were killed about 18 h after their last injection, hence it is possible that the effect might have been worn out in the brain.

Morphological analyses

Cerebellar vermis

In this study to estimate the changes in the population of the PCs we quantified their numbers (density) per millimeter of Purkinje cell layer (N_L). The two-way ANOVA combined analysis of four zones of the vermis (anterior zone, central zone, posterior zone and nodular zone; Figs 4, 5A) showed an overall significant decrease in the density of PCs in the experimental animals compared to control (F=83.96, p<0.0001). We also found significant increase in the PC density in the experimental group of mice treated with phenylbutyrate (EPB) (F=14.69, p<0.0001) compare to control one. Specifically, significant increase of density of PCs in EPB animals was observed in the anterior zone of the cerebellum (p=0.0001) (Fig. 5A). In contrast, there was no significant difference in the number of PCs between two control groups (saline injection – CSA and phenylbutyrate injection – CPB) (p=0.314).

The analyses of four zones of the vermis (anterior zone, central zone, posterior zone and nodular zone) showed an overall significant increase of the average cell size (cross-sectional area) of the PCs in the both groups of the experimental animals (ESA and EPB) compared to the control CSA and CPB groups. (p<0.0001) (Fig. 5B). This increase reached statistically significant levels in the anterior and posterior zones but not in the nodular zone of the vermis. However, a significant decrease of the PC size of the anterior and posterior zones was found in the EPB compared to ESA (p<0.0001) (Fig. 5B), thus demonstrating the reduction of the average PC soma size by PB. In contrast, the phenylbutyrate treatment had no effect on the PC size in control mice (CSA *vs.* CPB; p=0.8573).

Anterior zone

In the saline-injected experimental PDC-deficient (ESA) mice, the number (density) of PCs per millimeter of Purkinje cell layer (N_L) was markedly decreased (~38%) in comparison to the brains of the control saline-injected (CSA) group (51.1±2.6 *vs.* 82.3±3.3, respectively; p<0.0001) (Fig. 5A). In the PDC-deficient mice treated with phenylbutyrate (EPB), there was no significant difference in the number of neurons (71.6±4.8) compared to the CSA group (82.3±3.3) suggesting a reversal of the genetic effect. Interestingly, the cell size of PCs in the ESA group increased significantly (~50%) compared to the CSA group (281±4.3 μm^2 and 187.5±2.2 μm^2, respectively) (Fig. 5B; p<0.001). Between the ESA and EPB groups, there was a significant decrease (~26%) in the cell size of PCs in the EPB group (281±4.3 μm^2 and 222.7±3.5 μm^2, respectively; p<0.0001) (Fig. 5B).

Posterior zone

In the ESA group the number (density) of PCs per millimeter of Purkinje cell layer (N_L) was reduced (~28%) in comparison to the CSA group (40±3.9 *vs.* 55.7±5.1, respectively; p<0.0001) (Fig. 5A). A significant increase (~32%) in the number of PCs per millimeter of Purkinje cell layer in the EPB group was observed compared to the ESA group (58.8±7.3 *vs.* 40±3.9, respectively; p<0.05) (Fig. 5A). Consequently, in the EPB group, the number of PCs (58.8±7.3) normalized to the level of the CSA group (55.7±5.1) (Fig. 5A). The cell size of PCs increased (+36.6%) in the ESA group in comparison to the CSA group (251.1±3.8 μm^2 and 185.2±2.3 μm^2, respectively p<0.0001) (Fig. 5B). A significant decrease (~25%) was found in the EPB group compared to the ESA group (200.2±3.6 μm^2 *vs.* 251±3.8 μm^2, respectively; p<0.001). In the EPB group the size of PCs was still significantly different than in the CSA group (200.2±3.6 μm^2 *vs.* 185.2±2.3 μm^2, respectively; p<0.0001 (Fig. 5B).

Central zone

In the ESA group, the density of PCs was decreased (~27%) in comparison to the CSA group (52.6±3.6 *vs.* 72±5.2; p<0.0001) (Fig. 5A). The phenylbutyrate treatment had no effect on either the control or experimental mice. The difference (~20%) in the number of PCs between the EPB (43.5±4.4) and the ESA group (52.6±3.6) did not reach the statistical significance (p=0.97). The PC numbers in the EPB group (43.5±4.4) remained significantly lower (~40%; p<0.0001) than in the CSA group (72±5.2). The cell morphometric analysis of the same Nissl-stained sections showed that the size of PCs was significantly increased in the ESA compared to the CSA group (214.5±3.2 μm^2 and 178.0±3.7 μm^2, respectively; p<0.0001) (Fig. 5B). Additionally, phenylbutyrate had no effect on the average size of PCs in the central zone [the CSA *vs.* CBP (p=0.953) and the ESA *vs.* ESB groups (p=0.998)] (Fig. 5B).

Nodular zone

In the ESA group, the average density of PCs per millimeter of Purkinje cell layer (N_L) was markedly re-

duced (-53%) compared to the CSA group (36.2±1.9 *vs.* 83±9.1, respectively; $p<0.0001$) (Fig. 5A). However, there was no significant effect of phenylbutyrate administration in the control and PDC-deficient mice. The PC density in the EPB group remained lower (-55%) compared to the CSA group (37.3±7.4 *vs.* 83±9.1, respectively; $p<0.0001$) (Fig. 5A). The average cell size of PCs in the ESA group was significantly larger (~30%; $p<0.0001$) than in the CSA group (233.3±6 μm^2 and 183.6±3.2 μm^2, respectively) (Fig. 6). The average cell size of the PCs were not affected by the phenylbutyrate treatment in either the control or the deficient mice (Fig. 5B).

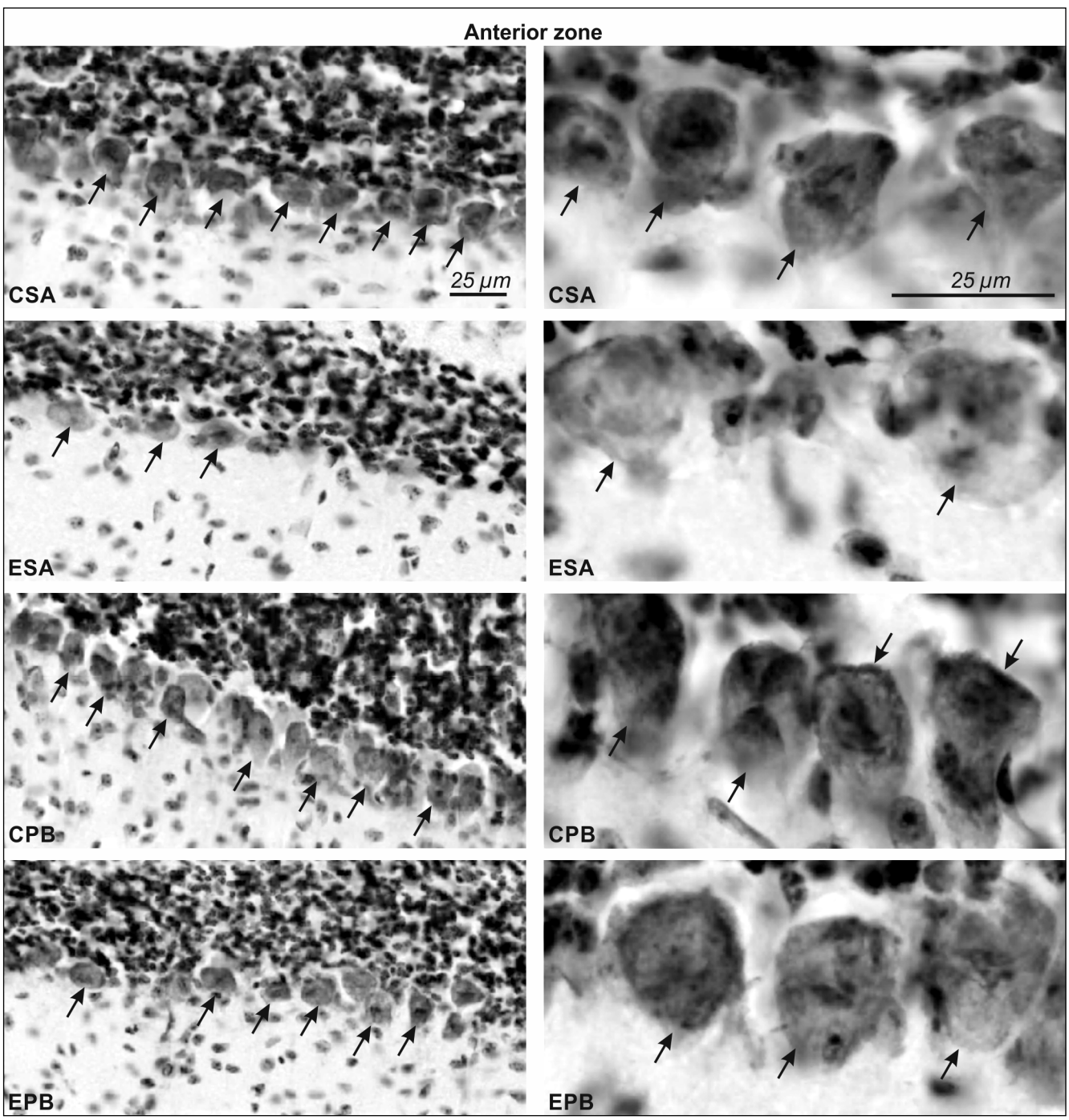

Fig. 4. Cresyl-violet (Nissl) staining photomicrographs (shown in black) of Purkinje cells (arrows). The figure shows the differences in the number (density) (left side) and cross-sectional area (cell size) (right side) of Purkinje cells between the control saline-injected (CSA) group and saline-injected PDC-deficient mice (ESA) with comparison to the PDC (EPB) and control (CPB) animals treated with phenylbutyrate in the anterior zone of the cerebellar vermis (scale bare = 25 μm).

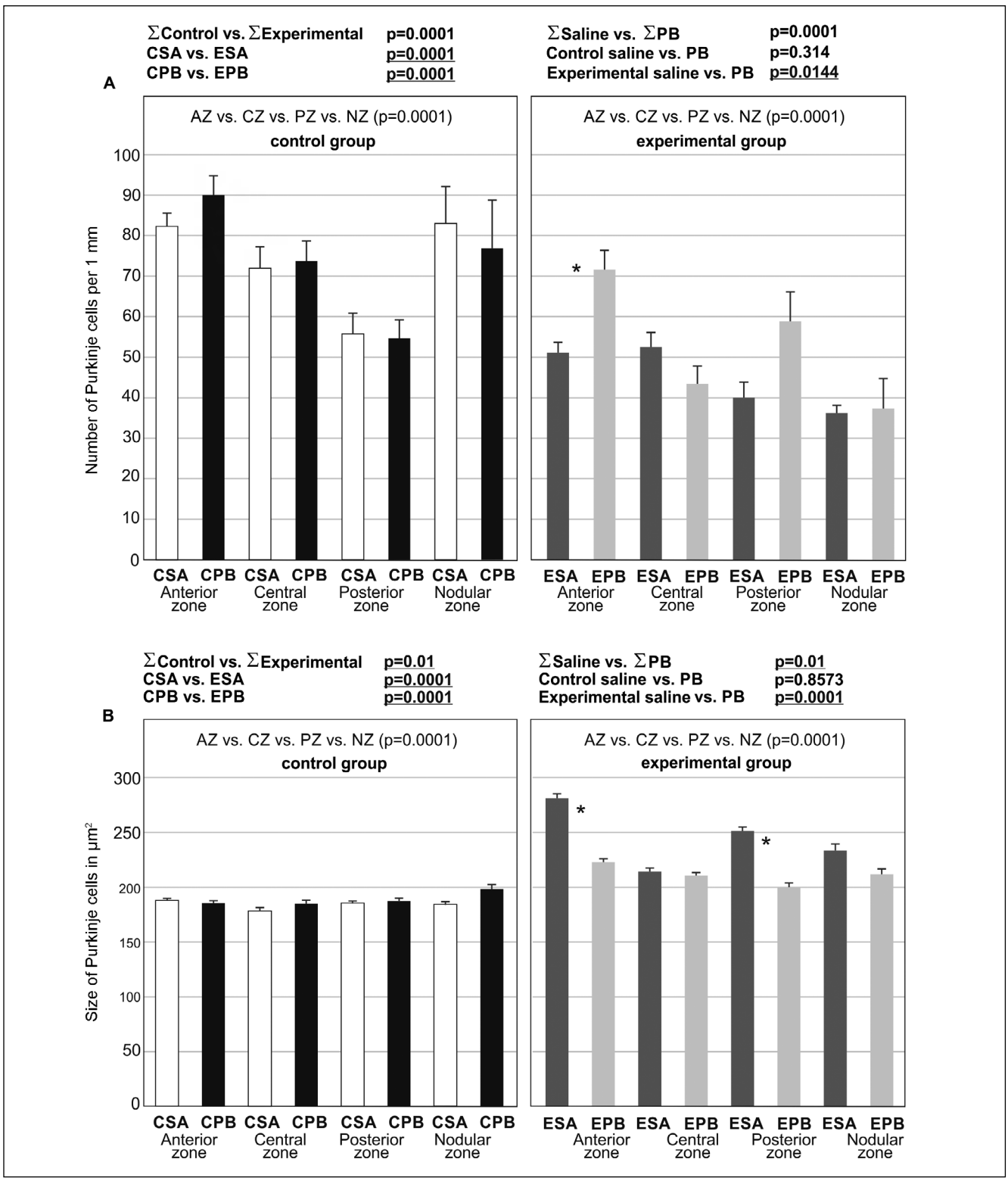

Fig. 5. The average density (number) (A) and the average cross-sectional area (cell size) (B) of Purkinje cells in the cerebellar vermis. (A) Significance was evaluated by Fisher test: the bar graph shows the data in control (left side) (MANOVA Fisher test F=83.96, df=1, ANOVA Fisher test F=8.75, df=3) and experimental groups (right side) (MANOVA Fisher test F=14.69, df=1, ANOVA Fisher test F=7.77, df=3). (B) Significance was evaluated by Fisher test: the bar graph shows the data in control (left side) (MANOVA Fisher test F=695.05, df=1, ANOVA Fisher test F=2.17, df=3) and experimental groups (right side) (MANOVA Fisher test F=102.64, df=1, ANOVA Fisher test F=46.02, df=3). Data are means ± S.E., * represents a significant difference between the animals treated with phenylbutyrate and non-treated in studied regions. Totally 1363 randomly chosen test areas were analyzed.

The cerebellar hemispheres

Two-way ANOVA analyses showed an overall statistically significant difference in the density (cell number) of PCs in the cerebellar hemispheres caused by PDC deficiency (for the factor experimental/control F=294.28, p<0.0001), an overall effect of the phenylbutyrate treatment (for drug/saline factor F=43.37, p<0.0001). However, we found no interaction between the phenylbutyrate effect and the PDC deficiency condition (F=0.88, p=0.3490). Thus, the effect of phenylbutyrate was similar both in the PDC-normal, control and the PDC-deficient, experimental, mice (Fig. 6A). There was a significant difference in the number of PCs between the two control groups (CSA and CPB) (p<0.026) (Fig. 6A).

The two-way ANOVA analysis showed an overall statistically significant difference in the cell size (cross-sectional area) of neurons between PDC-normal and PDC-deficient mice (for the factor experimental/control F=160.56, p<0.0001), and the overall significant effect of phenylbutyrate (for drug/no drug factor F=305.32, p<0.0001). There was a significant interaction of the two factors mentioned (F=53.07, p<0.0001) (Fig. 6B), thus the effect of phenylbutyrate was different in control, PDC-normal, and experimental (PDC-deficient) mice. The two-way ANOVA analysis of four zones of the hemispheres (paramedian lobule, Crus1, Crus2 and simple lobule) showed a significant increase of the cell size of the PCs between the experimental and the control mice (F=160.56, p<0.0001) as well as its decrease in the phenylbutyrate-treated animals (F=305.32, p<0.0001) (Fig. 6B). In experimental animals the phenylbutyrate administration significantly reduced the average cell size of PCs in all parts of the hemisphere (p<0.0001), however, the PC areas in the EPB mice were still significantly larger compared to the CSA mice (p<0.0008). Thus, the genotype-related changes were not fully reversed by phenylbutyrate.

There was significant interaction between the PDC condition and the phenylbutyrate effect (F=4.54 and p<0.0001). In both the PDC-deficient mice (EPB) and the control PDC-normal mice (CPB), phenylbutyrate reduced significantly the average PC cell size (p<0.0001) in all regions of the hemisphere (Fig. 6B).

Paramedian lobule

In the ESA group, the number (density) of PCs per millimeter of Purkinje cell layer (N_L) was significantly decreased (~23%) compared to the CSA group (28.2±0.8 *vs.* 36.9±0.9, respectively; p<0.0001) (Fig. 6A). The number of neurons in the EPB group did not differ significantly from the CSA group (33.5±1 and 36.9±0.9, respectively) (Fig. 6A). Significantly, in the EPB group the number of PCs increased (15.8%) compared to the ESA group (33.5±1 *vs.* 28.2±0.8, respectively; p=0.0195) (Fig. 6A). The cell size (cross-sectional area) of PCs in the ESA group was significantly larger than in the CSA group (219.4±4.7 μm^2 and 190.5±3.9 μm^2, respectively; p<0.0001) (Fig. 6B). There was a significant phenylbutyrate-induced decrease in CPB compared to the CSA group (166.1±3.4 μm^2 and 190.5±3.9 μm^2, respectively; p=0.0002) (Fig. 6B). The cell size of PCs in the EPB group was similar to that in the CSA group (184.4±4.5 μm^2 and 190.5±3.9 μm^2). Whereas, a significant decrease (~19%) in the size of PCs in the EPB group was observed compared to the ESA group (184.4±4.5 μm^2 and 219.4±4.7 μm^2, respectively; p<0.0001) (Fig. 6B).

Simple lobule

In the ESA group, the density of PCs per millimeter of Purkinje cell layer (N_L) was reduced (~31%) compared to the CSA group (30.7±1.2 *vs.* 44.3±1, respectively; p<0.0001) (Fig. 6A). The PC densities did not differ significantly between the CSA and CPB groups and also between the EPB and ESA groups (Fig. 6A). However, the number of PCs in the EPB mice remained lower than in the CSA mice (35.6±1 *vs.* 44.3±1, respectively; p<0.0001) (Fig. 6A). The size of PCs in the ESA group was significantly larger than in the CSA group (240.9±5.2 μm^2 and 201.1±4.5 μm^2, respectively; p<0.001) (Fig. 6B). Interestingly, there was a significant decrease in the cell size (cross-sectional area) of PCs between CSA and CPB groups (201.1±4.5 μm^2 and 174.4±3.8 μm^2, respectively; p<0.0001) and between the EPB and ESA groups (~26%) (191.1±4.2 μm^2 *vs.* 240.9±5.2 μm^2, p<0.0001) (Fig. 6B). The size of neurons in the EPB group became similar to that in the CSA group (191.1±4.2 μm^2 and 201.1±4.5 μm^2, respectively) (Fig. 6B).

Crus 1

In the ESA mice the density of PCs per millimeter of Purkinje cell layer was reduced compared to the CSA group (29.1±0.8 *vs.* 45.6±1.2, respectively; p<0.001) (Fig. 6A). In the EPB mice, ~24% decrease was seen in the PCs density compared to the CSA group (34.5±1.1 *vs.* 45.6±1.2, respectively; p<0.001). A significant increase (~15.6%) in the EPB was observed relative to the ESA group (34.5±1.1 *vs.* 29.1±0.8, respectively; p<0.0014) (Fig. 6A).

The cell size of PCs increased significantly (~23%) in the ESA mice compared to the CSA group (222.4±4.5 μm^2 and 180.4±4 μm^2, respectively; p<0.0001) (Fig. 6B). Interestingly, in this region of the cerebellum a significant (p<0.0001) decrease in cell size of PCs in the CPB group

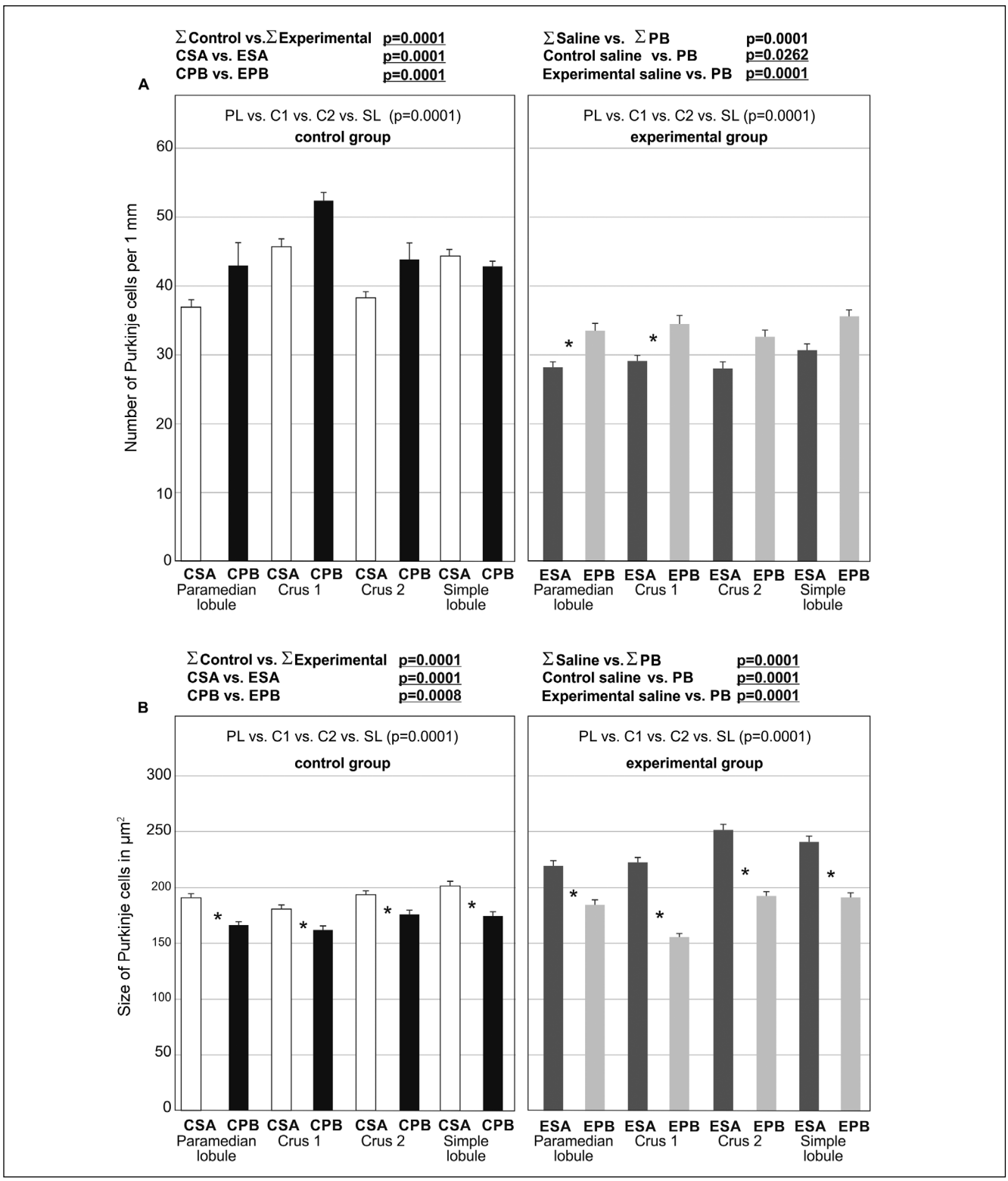

Fig. 6. The average density (number) (A) and the average cross-sectional area (cell size) (B) of Purkinje cells in the cerebellar hemisphere. (A) Significance was evaluated by Fisher test: the bar graph shows the data in control (left side) (MANOVA Fisher test F=294.28, df=1, ANOVA Fisher test F=12.00, df=3) and experimental groups (right side) (MANOVA Fisher test F=43.37, df=1, ANOVA Fisher test F=47.70, df=3). (B) Significance was evaluated by Fisher test: the bar graph shows the data in control (left side) (MANOVA Fisher test F=160.56, df=1, ANOVA Fisher test F=7.24, df=3) and experimental groups (right side) (MANOVA Fisher test F=305.32, df=1, ANOVA Fisher test F=21.80, df=3). Data are means ± S.E., * represents a significant difference between the animals treated with phenylbutyrate and non-treated in studied regions. Totally 838 randomly chosen test areas were analyzed.

was found compared to the CSA mice (162±3.6 μm^2 *vs.* 180.4±4 μm^2, respectively) (Fig. 6B). In the EPB mice, the size of the PCs was smaller than in the CSA group (155.7±3.1 μm^2 *vs.* 180.4±4 μm^2, respectively; p<0.0001). Treatment of the PDC-deficient mice with phenylbutyrate reduced significantly the cell size of PCs (~43%; p<0.0001) (ESA and EPB: 222.4±4.5 μm^2 and 155.7±3.1 μm^2, respectively).

Crus 2

In the ESA mice the density of PCs per millimeter of Purkinje cell layer (N_L) was smaller (~27%) compared to the CSA (28.1±0.8 *vs.* 38.2±1.2, respectively) (p<0.0001) (Fig. 6A). There was no significant difference in the number of PCs between the CSA and CPB control groups and between the EPB and the ESA groups (Fig. 6A). A significant decrease (~14%) in the number of PCs in the EBP group was observed compared to the CSA group (32.6.±1.2 and 38.2±1.2, respectively; p=0.0262). In the same Nissl-stained sections the average cell size of PCs was increased (~30%) in the ESA mice in comparison to the CSA group (251.5±5.1 μm^2 and 193.3±3.7 μm^2, respectively; p<0.0001) (Fig. 6B). Additionally, there was a significant difference in the size of PCs between CSA and CPB groups (193.3±3.7 μm^2 and 176±3.7 μm^2, respectively; p<0.0001) (Fig. 6B). The size of neurons in the EPB group was similar to that seen in the CSA group (192.5±3.9 μm^2 *vs.* 193.3±3.7 μm^2, respectively). A significant decrease (~30%) in the EBP mice was found compared to the ESA group (192.5±3.9 μm^2 and 251.5±5.1 μm^2, respectively; p<0.0001).

DISCUSSION

Previously published histological analyses of the brain sections from both the brain-specific and systemic-specific murine models of PDC-deficiency revealed brain structural defects such as disordered neuronal cytoarchitecture in grey matter, disorganization of fibers in white matter and reduction in the total PCs number as well as their dendritic arbors in the cerebellum (Pliss et al., 2004; 2013). The results reported in the present study support and extend the previous findings showing the alterations in both the cell number and cell size of PCs in different regions of the cerebellar cortex. In earlier reports, the treatment of phenylbutyrate was tested on PDC-deficient human fibroblasts and in a PDC-deficient zebra fish model (Brockerhoff et al., 1998; Ferriero et al., 2013). These studies have shown that phenylbutyrate increases the PDC activity in patients' fibroblasts and reverses the effects of PDC deficiency in the zebra fish model (Brockerhoff et al., 1998; Ferriero et al., 2013). Here we show for the first time in the mouse model that the postnatal administration of phenylbutyrate variably lessened the effects of PDC deficiency on Purkinje cell numbers and the cell size in different regions of the cerebellum. This variability may be related to the different timing of neurogenesis as well as the maturation of these cells in the cerebellum (Yuasa et al., 1991; Komuro, 2013).

In the present study, a *Cre* recombinase transgene driven by the nestin-promoter began to express by E10.5 in precursors of neurons and glia (Graus-Porta et al., 2001). Hence, the deletion of the *Pdha1* gene was initiated in the brain from E11-E13 and continued throughout the remaining fetal period and in the early postnatal period (until day 35 in the present study) during which the brain maturation is nearly completed. In our study, PDC deficiency reduced the density of PCs in the investigated regions of the cerebellar cortex. Interestingly, we observed a tendency for different degree of the loss of PCs due to its location in the cerebellum. In the cerebellar vermis the mean cellular loss was ~37% while in the cerebellar hemispheres it was ~26%. In the vermis the largest loss of neurons was observed in the nodular zone (53%) whereas in the anterior zone it was ~38%. Reduction of the cell density in the investigated regions of the cerebellar cortex in the PDC-deficient mice was accompanied by an increase in their soma size.

Evidence from cell and animal-based models suggest that the loss of PCs may be the result of abnormal development and related to early changes in PC physiology. In several disorders (e.g. ataxia, fetal alcohol syndrome, autism, Niemann-Pick disease, metabolic disease) (Parvizi et al., 2007; Schmahmann et al., 2007; Tavano et al., 2007; Reeber et al., 2013; Lawrenson et al., 2018), pathologic changes in PCs and a substantial loss of these neurons resulted in cerebellar atrophy and neurological symptoms.

In the present study a significant decrease in PCs density was observed in the vermis of cerebellum compared to the cerebellar hemispheres. The explanation for these differences could possibly lay in the duration of prolonged influence of pathological process on the earlier developed neurons for 'older' part of the cerebellum *vs.* the neurons originating later. As mentioned in the introduction, anterior-posterior and medial-lateral PC organization is established during development and is related to the timing of their birth. During development PCs form more than 50 distinct clusters, each of them with unique molecular characteristic. Clusters transform to sagittal stripes as the cerebellum expands along the anterior-posterior axis due to granular neuron progenitor cells proliferation and inward migration of granular neurons changing the multicellular Purkinje layer into

a PC monolayer. Furthermore, our earlier colocalization studies for BrdU and Neun revealed reduced proliferation and lower rate of differentiation in PDC-deficient mice in the both granular cells as well as PCs (Pliss et al., 2013), and this could explain the observed losses of PCs in the cerebellum in the present study.

The loss of PCs in the cerebellar cortex in the PDC-deficient mice was accompanied by an increase in the size of their cell soma. It is documented that the neuronal soma size is related to the number and size of the dendrites as well as the axon (Brannstrom et al., 1992a; 1992b). In the PDC-deficient mice, the increase in PC soma observed in the present study appears to be inversely related to their diminished dendritic arbors shown in our earlier report (Pliss et al., 2013). These changes may stem from the loss of Purkinje neurons and development of the adaptive neuronal modifications. Such adaptive changes as an increase of cell body size and a decrease of dendritic arborization were observed after lesion-induced changes in different regions of the brain (Gelfo et al., 2016). It is noteworthy that these authors also observed differences in PC morphology between vermis and cerebellar hemispheres (Gelfo et al., 2016).

As stated in the introduction, at present there is no effective treatment for PDC deficiency. Administration of high-fat, ketogenic diets, supplementation of high doses of thiamine (Blass et al., 1970; Wexler et al., 1997; Rubio-Gozalbo et al., 1999; Jankowska-Kulawy et al., 2014) and occasional administration of dichloroacetate (Preiser et al., 1990; Stacpoole et al., 2006) are commonly employed. However, none of these methods is fully effective and does not result in improvements of neurological problems and other clinical outcomes. Recent reports on human fibroblasts from PDC-deficient patients (Ferriero et al., 2013) and in a zebra fish model of PDC deficiency (Brockerhoff et al., 1995; 1998) indicate that phenylbutyrate may be a treatment option for the PDC deficiency. Earlier we reported that PDC deficiency adversely impacted the development of cellular structures in several different regions of the brain (Pliss et al. 2004; 2007). Hence, it is likely that administration of phenylbutyrate could also be effective in lessening the ill effects of PDC deficiency in other regions of the brain. This, however, would have to be dealt in any follow-up investigations. Sodium phenylbutyrate is routinely used to treat genetic defects in the urea cycle (Roy et al., 2012). Administration of phenylbutyrate to control mice during early postnatal growth (from postnatal day 2 to day 35) did not cause significant changes in the PC density or the cell size in the investigated areas of cerebellar cortex indicating lack of adverse effects of phenylbutyrate administration on the development of cerebellar PC population.

Phenylbutyrate treatment variably increased cell density (up to 47.1%) in the tested cerebellar regions of the EPB group and thus might diminish the adverse effect of PDC deficiency. The increased neuronal numbers were especially pronounced in the anterior (40%) as well as posterior (47.1%) zones of the vermis. However, in some cerebellar regions, e.g. the nodular zone, phenylbutyrate had no effect on the density of neurons. These different effects of phenylbutyrate could potentially related to the fact that the cells in this region are the oldest neurons in the cerebellum, and many might have died before the phenylbutyrate treatment was initiated. At the same time the cell size decreased in phenylbutyrate-treated animals in all studied regions, however, observed changes were different in specific areas of the cerebellum. The largest decrease in neuronal size in the phenylbutyrate-treated PDC-deficient mice (EPB) compared to the non-treated ESA mice were observed in most of the cerebellar regions, except the nodular and central zones.

There are reports describing beneficial effects of phenylbutyrate for several diseases in addition to PDC deficiency. Therapeutic effect of sodium phenylbutyrate on populations of dopaminergic neurons was described by Roy et al. (2012) in both acute and chronic 1-methyl-4-phenyl-1,2,3,6-tetrahydropyridine (MPTP) models of Parkinson's disease. MPTP intoxication caused approximately 75% loss of the substantia nigra dopamine neurons compared with the saline-injected control group. However, in MPTP-injected mice treated with sodium phenylbutyrate, less reduction in the loss of numbers of dopaminergic neurons was noted. Furthermore, sodium phenylbutyrate provided protection against deficits in the levels of dopamine and its two main metabolites, namely dihydroxyphenylacetic acid and homovanillic acid, in the striatum region 1 week after the MPTP injection (Roy et al., 2012). Phenylbutyrate treatment reduced the neuroinflammation in multiple sclerosis cases (Dasgupta et al., 2003; Iannitti and Palmieri, 2011). Furthermore, administration of sodium phenylbutyrate decreased the neurologic symptoms in a mouse model featuring cerebral hypoxia-ischemia (Qi et al., 2004; Iannitti and Palmieri, 2011). Whether the protective effects of phenylbutyrate administration on the number and size of the cellular Purkinje cell population improve the cerebellar function in drug-treated PDC-deficient mice is not known. If any, it could also depend up on possible protective influence of phenylbutyrate administration on other regions of the brain. In reference to metabolic diseases, a recent study using both *in vivo* and *in vitro* experiments showed that phenylbutyrate reduced the plasma levels of neurotoxic branched-chain amino acids and their corresponding α-keto acids in maple syrup

urine disease patients (Brunetti-Pierri et al., 2011; Iannitti and Palmieri, 2011). Interestingly, phenylbutyrate was shown to exert a potential anti-tumor effect *in vitro* causing growth inhibition in several different types of cancer (Svechnikova et al., 2003; Yokota et al., 2004; Svechnikov et al., 2008; Iannitti and Palmieri, 2011). It should be noted that these effects are not mediated *via* the PDC/PDH kinases interaction.

It is of interest to note that large deletions in the *PDHA1* gene resulting in the absence of detectable PDHα protein in cultured fibroblasts were unresponsive to phenylbutyrate treatment (Ferriero et al., 2014). In contrast, fibroblasts from PDC-deficient patients with missense mutations in the *PDHA1* gene were responsive to phenylbutyrate treatment by increasing PDC activity (Ferriero et al., 2014). Of the four different PDH kinase isoenzymes (1 to 4), phenylbutyrate inhibited isoenzymes 1 to 3 only. This inhibition was exerted by phenylbutyrate but not by its metabolite (Ferriero et al., 2015). In the present study, we could not detect a significant effect of the phenylbutyrate on the levels of phospho-PDHα (PE1α) protein in brains from either PDC-normal or PDC-deficient mice. This result differs from that of Ferriero et al. (2013) who observed the phenylbutyrate-induced reduction in phospho-PDHα protein in PDC-normal adult mice. There are methodological differences (such as age of animals, route of phenylbutyrate administration, daily split doses, and tissue preparations) between their report (Ferriero et al., 2013) and the present study, and these differences may account for different outcomes. Additionally, it is possible that the observed effects of phenylbutyrate in some regions of the cerebellum in the PDC-deficient mice could be due to other known biochemical effects of phenylbutyrate, as discussed above. Irrespective of the mechanism(s) of the phenylbutyrate action on the cerebellar PC, the results of our study lend further support for the use of phenylbutyrate as a potential treatment for PDC deficiency.

CONCLUSIONS

PDC deficiency in children causes abnormalities in brain structure development and cerebral function. The results presented here show that PDC deficiency in heterozygous PDC-deficient female mice results in significant reduction in the Purkinje cell density and cell size in different areas of the cerebellum. Daily administration of phenylbutyrate in the immediate postnatal period variably reduced impairment in Purkinje cell populations in different regions of the cerebellum. Our *in vivo* findings lend support for a potential use of phenylbutyrate as a novel treatment for PDC deficiency.

ACKNOWLEDGEMENTS

This study was supported in part by US Public Health Service Grant R21NS093264.

The funder had no role in study design, data collection and analysis, decision to publish, or preparation of the manuscript. The authors thank Sylwia Scislowska of Medical University of Gdansk for assisting in preparation of several figures and Dr. Todd Rideout of the University at Buffalo for critical reading of the manuscript.

AUTHOR CONTRIBUTIONS

M.S.P., M.K.S., E.K.S, conceptual planning; M.S.P., M.K.S. and E.K.S. funding acquisition; I.K., S.M. E.K.S., M.K.S. and M.S.P. experimental designs; I.K. and S.M. animal experimentation; I.K., J.M., N.M., A.E. histological analyses; I.K., M.S.P., J.M. and S.M. writing parts of original draft; all authors reviewing and editing.

REFERENCES

Apps R, Hawkes R (2009) Cerebellar cortical organization: a one-map hypothesis. Nat Rev Neurosci 10: 670–681.

Apps R, Hawkes R, Aoki S, Bengtsson F, Brown AM, Chen G, Ebner TJ, Isope P, Jorntell H, Lackey EP, Lawrenson C, Lumb B, Schonewille M, Sillitoe RV, Spaeth L, Sugihara I, Valera A, Voogd J, Wylie DR, Ruigrok TJH (2018) Cerebellar modules and their role as operational cerebellar processing units. Cerebellum 17: 654–682.

Ayala P, Montenegro J, Vivar R, Letelier A, Urroz PA, Copaja M, Pivet D, Humeres C, Troncoso R, Vicencio JM, Lavandero S, Diaz-Araya G (2012) Attenuation of endoplasmic reticulum stress using the chemical chaperone 4-phenylbutyric acid prevents cardiac fibrosis induced by isoproterenol. Exp Mol Pathol 92: 97–104.

Blass JP, Avigan J, Uhlendorf BW (1970) A defect in pyruvate decarboxylase in a child with an intermittent movement disorder. J Clin Invest 49: 423–432.

Brannstrom T, Havton L, Kellerth JO (1992a) Changes in size and dendritic arborization patterns of adult cat spinal alpha-motoneurons following permanent axotomy. J Comp Neurol 318: 439–451.

Brannstrom T, Havton L, Kellerth JO (1992b) Restorative effects of reinnervation on the size and dendritic arborization patterns of axotomized cat spinal alpha-motoneurons. J Comp Neurol 318: 452–461.

Brockerhoff SE, Dowling JE, Hurley JB (1998) Zebrafish retinal mutants. Vision Res 38: 1335–1339.

Brockerhoff SE, Hurley JB, Janssen-Bienhold U, Neuhauss SC, Driever W, Dowling JE (1995) A behavioral screen for isolating zebrafish mutants with visual system defects. Proc Natl Acad Sci USA 92: 10545–10549.

Brown GK, Otero LJ, LeGris M, Brown RM (1994) Pyruvate dehydrogenase deficiency. J Med Genet 31: 875–879.

Brunetti-Pierri N, Lanpher B, Erez A, Ananieva EA, Islam M, Marini JC, Sun Q, Yu C, Hegde M, Li J, Wynn RM, Chuang DT, Hutson S, Lee B (2011) Phenylbutyrate therapy for maple syrup urine disease. Hum Mol Genet 20: 631–640.

Buckner RL (2013) The cerebellum and cognitive function: 25 years of insight from anatomy and neuroimaging. Neuron 80: 807–815.

Cross JH, Connelly A, Gadian DG, Kendall BE, Brown GK, Brown RM, Leonard JV (1994) Clinical diversity of pyruvate dehydrogenase deficiency. Pediatr Neurol 10: 276–283.

Dasgupta S, Zhou Y, Jana M, Banik NL, Pahan K (2003) Sodium phenylacetate inhibits adoptive transfer of experimental allergic encephalomyelitis in SJL/J mice at multiple steps. J Immunol 170: 3874–3882.

De Meirleir L (2013) Disorders of pyruvate metabolism. In: Handbook of clinical neurology (Dulac LM, Sarmat HB, Eds.). Elsevier 113: p. 1667–1673.

DeBrosse SD, Kerr DS (2016) Pyruvate dehydrogenase complex deficiency. In: Mitochondrial studies; Underlying mechanisms and diagnosis (Saneto RP, Parikh S, Cohen BH, Eds.). Academic Press: p. 93–101.

Ferriero R, Boutron A, Brivet M, Kerr D, Morava E, Rodenburg RJ, Bonafe L, Baumgartner MR, Anikster Y, Braverman E, Brunetti-Pierri N (2014) Phenylbutyrate increases pyruvate dehydrogenase complex activity in cells harboring a variety of defects. Ann Clin Transl Neurol 1: 462–470.

Ferriero R, Iannuzzi C, Manco G, Brunetti-Pierri N (2015) Differential inhibition of PDKs by phenylbutyrate and enhancement of pyruvate dehydrogenase complex activity by combination with dichloroacetate. J Inherit Metab Dis 38: 895–904.

Ferriero R, Manco G, Lamantea E, Nusco E, Ferrante MI, Sordino P, Stacpoole PW, Lee B, Zeviani M, Brunetti-Pierri N (2013) Phenylbutyrate therapy for pyruvate dehydrogenase complex deficiency and lactic acidosis. Sci Transl Med 5: 175ra131.

Gelfo F, Florenzano F, Foti F, Burello L, Petrosini L, De Bartolo P (2016) Lesion-induced and activity-dependent structural plasticity of Purkinje cell dendritic spines in cerebellar vermis and hemisphere. Brain Struct Funct 221: 3405–3426.

Graus-Porta D, Blaess S, Senften M, Littlewood-Evans A, Damsky C, Huang Z, Orban P, Klein R, Schittny JC, Muller U (2001) Beta1-class integrins regulate the development of laminae and folia in the cerebral and cerebellar cortex. Neuron 31: 367–379.

Grodd W, Hulsmann E, Ackermann H (2005) Functional MRI localizing in the cerebellum. Neurosurg Clin N Am 16: 77–99.

Grodd W, Hulsmann E, Lotze M, Wildgruber D, Erb M (2001) Sensorimotor mapping of the human cerebellum: fMRI evidence of somatotopic organization. Hum Brain Mapp 13: 55–73.

Harris RA, Bowker-Kinley MM, Huang B, Wu P (2002) Regulation of the activity of the pyruvate dehydrogenase complex. Adv Enzyme Regul 42: 249–259.

Hemalatha SG, Kerr DS, Wexler ID, Lusk MM, Kaung M, Du Y, Kolli M, Schelper RL, Patel MS (1995) Pyruvate dehydrogenase complex deficiency due to a point mutation (P188L) within the thiamine pyrophosphate binding loop of the E1 alpha subunit. Hum Mol Genet 4: 315–318.

Iannitti T, Palmieri B (2011) Clinical and experimental applications of sodium phenylbutyrate. Drugs R D 11: 227–249.

Jankowska-Kulawy A, Bielarczyk H, Ronowska A, Bizon-Zygmanska D, Szutowicz A (2014) Disturnbances of brain energy metabolism in thiamine deficiency. J Lab Diagn 50: 333–338.

Jankowski J, Miething A, Schilling K, Oberdick J, Baader S (2011) Cell death as a regulator of cerebellar histogenesis and compartmentation. Cerebellum 10: 373–392.

Johnson MT, Mahmood S, Hyatt SL, Yang HS, Soloway PD, Hanson RW, Patel MS (2001) Inactivation of the murine pyruvate dehydrogenase (Pdha1) gene and its effect on early embryonic development. Mol Genet Metab 74: 293–302.

Kaufmann P, Engelstad K, Wei Y, Jhung S, Sano MC, Shungu DC, Millar WS, Hong X, Gooch CL, Mao X, Pascual JM, Hirano M, Stacpoole PW, DiMauro S, De Vivo DC (2006) Dichloroacetate causes toxic neuropathy in MELAS: a randomized, controlled clinical trial. Neurology 66: 324–330.

Kelly RM, Strick PL (2003) Cerebellar loops with motor cortex and prefrontal cortex of a nonhuman primate. J Neurosci 23: 8432–8444.

Komuro Y, Kumada T, Ohno N, Foote KD, Komuro, H (2013) Migration in the cerebellum. Cellular migration and formation of neuronal connections. In: Comprehensive Developmental Neuroscience (Rubenstein JLR, Rakic P, Eds.). Academic Press, p. 281–297.

Lawrenson C, Bares M, Kamondi A, Kovacs A, Lumb B, Apps R, Filip P, Manto M (2018) The mystery of the cerebellum: clues from experimental and clinical observations. Cerebellum Ataxias 5: 8.

Leggio M, Olivito G (2018) Topography of the cerebellum in relation to social brain regions and emotions. In: The Cerebellum from Embryology to Diagnostic Investigations (Manto M, Huisman TAGM, Eds.). Elsevier, 154 p. 71-84.

Leto K, Arancillo M, Becker EB, Buffo A, Chiang C, Ding B, Dobyns WB, Dusart I, Haldipur P, Hatten ME, Hoshino M, Joyner AL, Kano M, Kilpatrick DL, Koibuchi N, Marino S, Martinez S, Millen KJ, Millner TO, Miyata T, Parmigiani E, Schilling K, Sekerkova G, Sillitoe RV, Sotelo C, Uesaka N, Wefers A, Wingate RJ, Hawkes R (2016) Consensus Paper: Cerebellar Development. Cerebellum 15: 789–828.

Levisohn L, Cronin-Golomb A, Schmahmann JD (2000) Neuropsychological consequences of cerebellar tumour resection in children: cerebellar cognitive affective syndrome in a paediatric population. Brain 123: 1041–1050.

Lissens W, De Meirleir L, Seneca S, Liebaers I, Brown GK, Brown RM, Ito M, Naito E, Kuroda Y, Kerr DS, Wexler ID, Patel MS, Robinson BH, Seyda A (2000) Mutations in the X-linked pyruvate dehydrogenase (E1) alpha subunit gene (PDHA1) in patients with a pyruvate dehydrogenase complex deficiency. Hum Mutat 15: 209–219.

Livak KJ, Schmittgen TD (2001) Analysis of relative gene expression data using real-time quantitative PCR and the 2(-Delta Delta C(T)) method. Methods 25: 402–408.

Matthews PM, Brown RM, Otero LJ, Marchington DR, LeGris M, Howes R, Meadows LS, Shevell M, Scriver CR, Brown GK (1994) Pyruvate dehydrogenase deficiency. Clinical presentation and molecular genetic characterization of five new patients. Brain 117: 435–443.

Miale IL, Sidman RL (1961) An autoradiographic analysis of histogenesis in the mouse cerebellum. Exp Neurol 4: 277–296.

Middleton FA, Strick PL (2001) Cerebellar projections to the prefrontal cortex of the primate. J Neurosci 21: 700–712.

Naito E, Kuroda Y, Takeda E, Yokota I, Kobashi H, Miyao M (1988) Detection of pyruvate metabolism disorders by culture of skin fibroblasts with dichloroacetate. Pediatr Res 23: 561–564.

Parvizi J, Joseph J, Press DZ, Schmahmann JD (2007) Pathological laughter and crying in patients with multiple system atrophy-cerebellar type. Mov Disord 22: 798–803.

Patel MS, Harris RA (1995) Alpha-keto acid dehydrogenase complexes: nutrient control, gene regulation and genetic defects. Overview. J Nutr 125: 1744S-1745S.

Patel MS, Kerr DS, Wexler ID (1992) Biochemical and molecular aspects of pyruvate dehydrogenase complex deficiency. International Pediatrics 7: 16–22.

Patel MS, Korotchkina LG (2003) The biochemistry of the pyrutate dehydrogenase complex. Biochem Mol Biol Edu 31: 5–15.

Patel MS, Roche TE (1990) Molecular biology and biochemistry of pyruvate dehydrogenase complexes. FASEB J 4: 3224–3233.

Paxinos G, Franklin KBJ (2013) Paxinos and Franklin's The Mouse brain in stereotaxic coordinates. Academic Press, Amsterdam.

Pliss L, Hausknecht KA, Stachowiak MK, Dlugos CA, Richards JB, Patel MS (2013) Cerebral developmental abnormalities in a mouse with systemic pyruvate dehydrogenase deficiency. PLoS One 8: e67473.

Pliss L, Mazurchuk R, Spernyak JA, Patel MS (2007) Brain MR imaging and proton MR spectroscopy in female mice with pyruvate dehydrogenase complex deficiency. Neurochem Res 32: 645–654.

Pliss L, Pentney RJ, Johnson MT, Patel MS (2004) Biochemical and structural brain alterations in female mice with cerebral pyruvate dehydrogenase deficiency. J Neurochem 91: 1082–1091.

Preiser JC, Moulart D, Vincent JL (1990) Dichloroacetate administration in the treatment of endotoxin shock. Circ Shock 30: 221–228.

Qi X, Hosoi T, Okuma Y, Kaneko M, Nomura Y (2004) Sodium 4-phenylbutyrate protects against cerebral ischemic injury. Mol Pharmacol 66: 899–908.

Reeber SL, Loeschel CA, Franklin A, Sillitoe RV (2013a) Establishment of topographic circuit zones in the cerebellum of scrambler mutant mice. Front Neural Circuits 7: 122.

Reeber SL, Otis TS, Sillitoe RV (2013b) New roles for the cerebellum in health and disease. Front Syst Neurosci 7: 83.

Robinson BH (2001) Lactic Acidemia: Disorders of Pyruvate Carboxylase and Pyruvate Dehydrogenase. In: The Metabolic and Molecular Basis of Inherited Disease (Scriver CR, Beaudet AL, Sly WS, Valle D, Eds.). McGraw-Hill, New York, Toronto, p. 2275–2295.

Robinson BH (2006) Lactic acidemia and mitochondrial disease. Mol Genet Metab 89: 3–13.

Roy A, Ghosh A, Jana A, Liu X, Brahmachari S, Gendelman HE, Pahan K (2012) Sodium phenylbutyrate controls neuroinflammatory and antioxidant activities and protects dopaminergic neurons in mouse models of Parkinson's disease. PLoS One 7: e38113.

Rubio-Gozalbo ME, Heerschap A, Trijbels JM, De Meirleir L, Thijssen HO, Smeitink JA (1999) Proton MR spectroscopy in a child with pyruvate dehydrogenase complex deficiency. Magn Reson Imaging 17: 939–944.

Schmahmann JD (2004) Disorders of the cerebellum: ataxia, dysmetria of thought, and the cerebellar cognitive affective syndrome. J Neuropsychiatry Clin Neurosci 16: 367–378.

Schmahmann JD, Weilburg JB, Sherman JC (2007) The neuropsychiatry of the cerebellum – insights from the clinic. Cerebellum 6: 254–267.

Shireman RB, Mace L, Davidson S (1984) Effects of dichloroacetate and glyoxylate on low density lipoprotein uptake and on growth of cultured fibroblasts. Proc Soc Exp Biol Med 175: 420–423.

Sokoloff L (1999) Energetics of functional activation in neural tissues. Neurochem Res 24: 321–329.

Srinivasan K, Sharma SS (2011) Sodium phenylbutyrate ameliorates focal cerebral ischemic/reperfusion injury associated with comorbid type 2 diabetes by reducing endoplasmic reticulum stress and DNA fragmentation. Behav Brain Res 225: 110–116.

Stacpoole PW, Kerr DS, Barnes C, Bunch ST, Carney PR, Fennell EM, Felitsyn NM, Gilmore RL, Greer M, Henderson GN, Hutson AD, Neiberger RE, O'Brien RG, Perkins LA, Quisling RG, Shroads AL, Shuster JJ, Silverstein JH, Theriaque DW, Valenstein E (2006) Controlled clinical trial of dichloroacetate for treatment of congenital lactic acidosis in children. Pediatrics 117: 1519–1531.

Stoodley CJ, Schmahmann JD (2018) Functional topography of the human cerebellum. In: The Cerebellum From Embryology to Diagnostic Investigation (Manto M, Huisman TAGM, Eds.). Elsevier. 154: p. 59–70.

Svechnikov K, Svechnikova I, Soder O (2008) Inhibitory effects of mono-ethylhexyl phthalate on steroidogenesis in immature and adult rat Leydig cells *in vitro*. Reprod Toxicol 25: 485–490.

Svechnikova I, Gray SG, Kundrotiene J, Ponthan F, Kogner P, Ekstrom TJ (2003) Apoptosis and tumor remission in liver tumor xenografts by 4-phenylbutyrate. Int J Oncol 22: 579–588.

Tavano A, Grasso R, Gagliardi C, Triulzi F, Bresolin N, Fabbro F, Borgatti R (2007) Disorders of cognitive and affective development in cerebellar malformations. Brain 130 : 2646–2660.

Triepels RH, van den Heuvel LP, Loeffen JL, Buskens CA, Smeets RJ, Rubio Gozalbo ME, Budde SM, Mariman EC, Wijburg FA, Barth PG, Trijbels JM, Smeitink JA (1999) Leigh syndrome associated with a mutation in the NDUFS7 (PSST) nuclear encoded subunit of complex I. Ann Neurol 45: 787–790.

Voogd J, Glickstein M (1998) The anatomy of the cerebellum. Trends Neurosci 21: 370–375.

Wexler ID, Hemalatha SG, McConnell J, Buist NR, Dahl HH, Berry SA, Cederbaum SD, Patel MS, Kerr DS (1997) Outcome of pyruvate dehydrogenase deficiency treated with ketogenic diets. Studies in patients with identical mutations. Neurology 49: 1655–1661.

White JJ, Sillitoe RV (2013) Development of the cerebellum: from gene expression patterns to circuit maps. Wiley Interdiscip Rev Dev Biol 2: 149–164.

White JJ, Sillitoe RV (2013) Postnatal development of cerebellar zones revealed by neurofilament heavy chain protein expression. Front Neuroanat 7: 9.

Wildgruber D, Ackermann H, Grodd W (2001) Differential contributions of motor cortex, basal ganglia, and cerebellum to speech motor control: effects of syllable repetition rate evaluated by fMRI. Neuroimage 13: 101–109.

Yokota N, Mainprize TG, Taylor MD, Kohata T, Loreto M, Ueda S, Dura W, Grajkowska W, Kuo JS, Rutka JT (2004) Identification of differentially expressed and developmentally regulated genes in medulloblastoma using suppression subtraction hybridization. Oncogene 23: 3444–3453.

Yuasa S. Kawamura K, Ono K, Yamakuni T, Takahashi Y (1991) Development and migration of Purkinje cells in the mouse cerebellar primordium. Anat Embryol 184: 195–212.